Dalton Transactions

Accepted Manuscript

ROYAL SOCIETY OF CHEMISTRY

www.rsc.org/dalton

Cite this: DOI: 10.1039/c0xx00000x

www.rsc.org/xxxxxx

ARTICLE TYPE

Elucidating the Structures and Cooperative Binding Mechanism of Cesium Salts to Multitopic Ion-Pair Receptor through Density Functional Theory Calculations

Biswajit Sadhu[(1)], Mahesh Sundararajan[(2)*], Gunasekaran Velmurugan[(3)] and PonnambalamVenuvanalingam[(3)]

Received (in XXX, XXX) XthXXXXXXXXX 20XX, Accepted Xth XXXXXXXXX 20XX
DOI: 10.1039/b000000x

Designing new and innovative receptors for the selective binding of radionuclides is central to nuclear waste management processes. Recently, a new multi-topic ion-pair receptor was reported which binds a variety of cesium salts. Due to the large size of the receptor, quantum chemical calculations on the full ion-pair receptors are restricted, thus the binding mechanism are not well understood at the molecular level. We have assessed the binding strengths of various cesium salts to recently synthesized multi-topic ion-pair receptor molecule using density functional theory based calculations. Our calculations predict that the binding of cesium salts to the receptor is predominantly occurs *via* cooperative binding mechanism. Cesium and anion synergistically assist each other to bind favorably inside the receptor. Energy decomposition analysis on the ion-pair complexes shows that the Cs salts are bound to the receptor mainly through electrostatic interactions with small contribution from covalent interactions for large ionic radii anions. Further, QTAIM analysis characterizes the importance of different inter-molecular interactions between the ions and the receptor inside the ion-pair complexes. The role of crystallographic solvent molecule contributes significantly by ~10 kcal mol^{-1} to the overall binding affinities which is quite significant. Further, unlike the recent molecular mechanics (MM) calculations, our calculated binding affinity trends for various Cs ion-pair complexes (CsF, CsCl and $CsNO_3$) are now in excellent agreement to the experimental binding affinity trends.

Introduction

Designing new ligands for the selective separation of harmful and toxic radionuclides such as cesium[1,2](Cs^{137}), strontium[3](Sr^{89}, Sr^{90}) and iodine[4,5](I^{129}, I^{131}) have gained significant interest to reduce the volume of generating nuclear fission products from nuclear power production and from nuclear reactor accidents like Chernoboyl[6] and Fukushima Diichi[7]. Post processing of these nuclear wastes using a selective ion probe remains to be the most challenging aspects of on-going nuclear strategies in the back-end of the fuel cycle. To this end, numerous experimental studies have been carried out to identify ligands suitable for selective extraction of radionuclide ions.

Notes
[1]*Radiation Safety Systems Division, Bhabha Atomic Research Centre, Mumbai – 400 085, India, Mumbai – 400 085, INDIA,*
[2]*Theoretical Chemistry Section, Bhabha Atomic Research Centre Mumbai – 400 094, India Tel.: +91 22 25593829, Fax: +91 22 25505151, E-mail: smahesh@barc.gov.in*
[3]*School of Chemistry, Bharathidasan University, Tiruchirappalli- 620 024*

Some notable host molecules include crown ether[8],calix[4]arene-crown-[6][9, 10] and calix crown[11-13]receptors, which are found to bind cesium cation (Cs^+) with high selectivity. On the other hand, pyridyl terminated tripodal amide receptor[14,15] and calix-pyrrole[16-18]are promising ligands to selectively bind various halide anions (F^-, Cl^- and I^-).

Further, in solvent extraction processes, the influence of counter ions is recognized to be an important and decisive factor to achieve better separation factor.[19,20] In this direction, several multi-topic ion-pair receptors have been synthesized. Particularly Sessler and co-workers[21-24] have pioneered in synthesizing many ion-pair receptors, which tend to enhance the binding through favourable cooperative effects. Interestingly, within the various ion-pair binding receptors, the binding mechanism of each ion-pair are unique from one receptor to another. For example, in the crown-6-calix[4]arene-capped calix[4]pyrrole, both cations and anions are observed to bind simultaneously to the host,[23] whereas in another one (calix[4]pyrrole-calix[4]arene), the ions bind through the sequential mechanism.[24]

Very recently, Kim et al.[25,26] reported yet another ion-pair receptor (calix[4]arene crown-[5] strapped with calix[4]pyrrole

moiety *via* glycol and aromatic linker) for the efficient extraction of Cs^+ *via* cation metathesis. This receptor is composed of three main cation binding sites, namely calix[4]arene-crown-5 (C), glycol site (G), the concave site of calix[4]pyrrole (P) and, two probable anion (X^-) binding sites namely convex side of calix[4]pyrrole (P) and outer sphere of the crown site(C) (figure 1). Hence, resulted in four distinguishable binding modes for the Cs salts in the receptor, namely C/P, G/P, P/P and C/C where first letter stands for cation binding site and later is for anion binding site (scheme 1). In conjunction with experimental data, theoretical gas phase calculations using molecular mechanics (MM) force fields were also carried out to gain more insights on the preferable binding mode.

Noticeably, MM calculations carried out in the gas phase for the above mentioned ion-pair receptor[25,26] failed to follow the experimental binding trends. For example, although the experimental data suggest the C/P binding mode is to be thermodynamically favourable for CsF and CsCl, MM calculations predict C/C and G/P binding modes. Further, the computational results do not shed light over the existence of positive allosteric effects in the ion-pair binding mechanism. An elucidation of such acting cooperative effects in the receptor at the molecular level is indeed very essential and can act as a test bed for synthesizing more efficient ion binding probe.

Quantum chemical calculations at the density functional theory (DFT) level are very popular and powerful method to investigate the binding preferences of various radionuclides to different hosts.[27-29]For instance, Boda et al investigated the selective binding of Cs^+ over Na^+ with macro cyclic calix-bis-crown ether.[27]Hill et al. studied the binding of various alkali metal cations to crown ether and its analogues.[28]However, apart from the aforementioned experimental investigations, owing to the large system size, quantum chemical calculations on these reported ion-pair receptors are very rare.[30]

Here, we have carried out DFT calculations on the ion-pair receptor of Kim. et al.[25,26]to unravel the structures and binding mechanism of Cs salts. Our present study focused to address the following intriguing questions,

(i) What are the binding affinities of anions and Cs^+ in the absence of their counterparts?
(ii) Which is the most preferable binding mode for cesium salts at this receptor and why?
(iii) To what extent, cation or anions assist each other in binding? and,
(iv) To what extent solvent molecules alter the binding affinity trend?

In addition to this, we have also carried out energy decomposition analysis (EDA) to determine the various contributions of interaction energy components into the total interaction energy. Besides, topological analysis using atoms in molecule (AIM) approach is performed to decipher the nature of inter-molecular interactions existing in the ion-pair complexes. These two tools have gained considerable attention to understand the nature of bonding present between the ions and the extractants.[31, 32]

Computational Details

The starting structures of the ion-pair receptor are taken from the reported X-ray structure of Kim et al.[25,26]We have considered various cesium-halide salts, viz. CsF (CCDC codes: 826578), CsCl (CCDC codes: 826574), CsBr and CsI along with$CsNO_3$ (CCDC codes: 826577) for complexation with the receptor. For CsBr and CsI, we have used the CsCl X-ray structure. All X-ray derived structures are further optimized using BP86 functional[33, 34]in conjunction with the def2-SV(P) basis set (denoted as B1 basis set).[35]Notably, this functional/basis set (BP86/de2-SV(P) was previously observed to produce accurate structural parameters.[36-39]The effect of long range electrostatic effects are taken into account by using the implicit COSMO solvation model (water as solvent; ε= 80).[40]The size of the system is very large (173-187 atoms), such that even with double ζ-basis set (1572 basis functions), the computation is very demanding. Thus, geometry optimizations with the larger basis sets are prohibitive. Nevertheless, to comment on the basis set dependency of the structure and energetics, a set of calculations are performed for [Receptor.CsCl] complex at the C/P binding mode using a basis set of triple ζ-quality[41, 42](TZVP, 2404 basis functions, denoted as B2 basis set) (ref SI, Table S1, S2). The obtained structural changes between def2-SV(P) and TZVP basis set are found to be negligible. Further, binding affinities are also observed to deviate only by 4 kcal mol^{-1} (ref SI, Table S2).

Moreover, the above complex is also optimized at gas phase as well as at ε=80 with and without Grimme's three-body dispersion correction term (denoted as D3 correction).[43] Noticeably, the optimized structural parameters with D3 corrections are observed to deviate more with respect to X-ray structure (ref SI, Table S1). The same is noted for the gas phase optimized structure at BP86/B1 level. Such alteration in geometry is found to be minimal in case of COSMO optimized structure at BP86/B1 level. The above results thus justify our applied DFT level (BP86/B1 using implicit solvation scheme (ε=80)) for geometry optimization.

Compared to BP86, hybrid B3LYP[44,45] performs better in energetics calculations.[46,47] Hence, Binding affinities are computed using dispersion corrected B3LYP(D3) functional with a B2 basis set on BP86/B1 pre-optimized structuresat ε=80. For Cs^+ and I^- ions, a def-TZVP basis set was used to describe the valance orbitals, whereas the core electrons were modelled via SD-ECP (replacing 46 electrons in the core)[48] pseudo potential. To speed up the calculations, a resolution of identity (RI or RIJCOSX) approximation[49-53]was applied by using corresponding auxiliary basis sets. Similar computational methodology was successfully used by us to benchmark the alkane binding to cucurbiturils with the experimental binding free energies [54] and also to describe binding mechanism of Cs^+ in fulvic acid.[55]

Due to large system size the harmonic frequency calculations on ion-pair receptor adducts are computationally very expensive. Further, the experimentally determined thermodynamic quantities suggests the binding of ion-pair to the receptor is enthalpy

driven,[25,26] hence our derived electronic binding affinities can be expected to correlate well with the experimental binding trend. All structural optimizations are performed using TURBOMOLE v 6.3.1[56] while energetics are computed using ORCA v 3.0 software.[57]

The nature of interactions present between Cs^+/X^- and the receptor have been analysed using BP86/B1 (ε=80) optimized structures by means of EDA as implemented in the ADF program package[58] based on the methods pioneered by Morokuma[59] and Ziegler[60] at a level of BLYP/TZ2P with ZORA. It should be noted that Pardue et al[62] reported that both BLYP and B3LYP functional predict similar EDA parameters. Thus for computational efficiency we chose BLYP/TZ2P method for the present study. The total interaction energy (ΔE_{int})between the two fragments is calculated using the following equation,

$$\Delta E_{int}(\zeta) = \Delta E_{elstat}(\zeta) + \Delta E_{pauli}(\zeta) + \Delta E_{orb}(\zeta) \quad (1)$$

and, the percentage covalency have been calculated using the equation 2,

$$[\Delta E_{orb}(\zeta)/(\Delta E_{elstat}(\zeta) + \Delta E_{orb}(\zeta))] \times 100 \quad (2)$$

where, ΔE_{elstat} (ζ) and ΔE_{pauli} (ζ) represents the electrostatic and repulsive interaction energy contributions between the fragments respectively. ΔE_{orb} (ζ) is the stabilizing energy arises from the orbital contributions and thus represents the strength of covalent bonding between the fragments.

Further, the quantum theory of atoms in molecule (QTAIM) was applied to depict the topological properties of the most favourable [Receptor-Cs^+X^-] complexes. QTAIM analysis, pioneered by Bader and co-workers characterizes bonding and non-bonding interactions of atoms in terms of the electron density $\rho(r)$, Laplacian of the electron density L(r), kinetic energy density H(r) and a potential energy to the Lagrangian kinetic energy ratio (|V(r)/G(r))|.[63]For instance, the presence of a (3, -1) critical point in QTAIM topography represents a chemical bond between two atoms and are called as the bond critical points (BCPs) where the shared electron density reaches a minimum, whereas a critical point with (3, +1) and (3, +3) signatures identify a ring structure (RCP) and cage critical point (CCP) in the molecular system. The $\rho(r)$ values at the BCPs is related to the strength of the bonds.[64]In this study, QTAIM calculations are performed at BP86/B2 level[65] using AIM2000 package.[66]

Results and Discussion

(a) Solvation of Ions:

The preferential binding of ions to the receptor is known to be modulated by dehydration penalty of ions. From the earlier studies,[27,29, 67-69] it is apparent that a primary hydration number of six can be considered for the halide ions and for Cs cation. Topol et al.[67] demonstrated that the primary hydration shell of F^-, Cl^- and Br^- contains six water molecules. DFT studies by both Dang et al.[68] and Ali et al.[69] predicteda partially solvated structures for I^- and Cs^+ to be the most stable species. Recently, we have also used hexa-hydrated halide ions towards understanding the ion-host interaction at the molecular level.[29]Similarly, for nitrate, Bodaet al.[27] used hexa hydrated structure in their previous quantum chemical calculation. The same solvated models have been used here in our study. To validate the solvation model, we have calculated the hydration free energies of all ions which are indeed found to be close with the experimentally derived values (ref SI, Figure S1 and Table S3),[70]and in particular the trends are excellently reproduced. Thus the chosen methods BP86/B1 for geometry optimizations within the implicit COSMO solvation model and B3LYP-D3/B2 for energetics are accurate enough for the present study.

(b)Binding of Cesium to Receptor

The receptor bears three binding sites for Cs^+ namely, 'C', 'G' and 'P' site (figure 1). Cs^+cation binding affinity to the receptor have been calculated using the following equation:

$$E_{[Receptor]} + E_{[Cs+.(H2O)6]} \rightarrow E_{[Receptor\text{-}Cs+]} + E_{[(H2O)6]} \quad (3)$$

For the 'C' and 'G' sites, the calculated binding affinities are -15 kcal mol^{-1} and -13 kcal mol^{-1} respectively.Among the three binding sites, Cs^+ binding to the 'P'-site is least favourable (B.E ~-7 kcal mol^{-1}) (Table 1). Hence, 'C' and 'G' sites act as the primary binding site for Cs^+ in absence of anion.

Cs^+ at the 'C' site interacts with crown-5 oxygen atoms through strong electrostatic interaction (Cs-O_{crown}- 2.93-3.10 Å). Aromatic moieties of calix-[4]-arene are also found to interact with Cs^+ through cation-π interaction in the C site (Cs-Arene-3.45-3.51 Å). However, in 'G' site, in addition to cation-π interaction with the calix[4]arene moiety(Cs-Arene-3.54-3.74 Å), two ethylene glycol spacers (Cs-O_G- 3.06-3.56 Å) further provide favourable electrostatic interaction whereas larger space of the cavity reduces steric hindrance. Finally, for the 'P'site, pyrrole rings of calix[4]pyrrole unit interacts weakly with Cs^+ *via* cation-π interaction (Cs-N_P-3.66-3.73 Å) and thus lead to minimal binding affinity (only 7 kcal mol^{-1}) and energetically less favorable as compared to 'C' and 'G' site.

(c) Binding of Anions to Receptor

The chosen anions (X= F^-, Cl^-, Br^-, I^- and NO_3^-) can bind either at 'P' or at the outer sphere of 'C' site of the receptor through hydrogen bonding (table 2).Anion (X^-) binding affinities to the receptor have been calculated using the following equation,

$$E_{[Receptor]} + E_{[X\text{-}.(H2O)6]} \rightarrow E_{[Receptor\text{-}X\text{-}]} + E_{[(H2O)6]} \quad (4)$$

In site 'C', anions can only interact with the methylene hydrogen atoms through weak hydrogen bonding (F^--H > 2 Å), whereas at the 'P' site, a strong hydrogen bonding (F^-...H-$N_{pyrrole}$-1.68-1.70 Å, I^-...H-$N_{pyrrole}$-2.58-2.63 Å) is noted. These variations in the geometry lead to favorable binding affinity at the 'P' site (~-5 kcal $mol^{-1}$for F^-) but unfavorable binding is noted for the 'C' site (>+5 kcal mol^{-1}). For large I^- anion, both the sites are found to be unfavorable. The computed bond lengths are consistent with the structural parameters of previously reported computational study for calix[4]pyrrole-halide system[71,72]and with reported experimental data (F^-...H-N:1.64 Å, I^-...H-N:2.69 Å).[73]

Evidently, electronegativity and hydration energy of anions

play an important role in their selective binding at the'P' site. Interestingly, despite having highest electronegativity, F^- is noted to have a lower binding affinity than $Cl^-$and Br^-. This can be attributed to the strong solvation nature of the F^- at water medium which increases the desolvation energy barrier for F^-. Notably, earlier experiments by Kim et al.[26]also observed no complexation of F^- with the receptor in the more polar medium. For the 'P' site, the strength of anion binding decreases as follows,

$Cl^- > Br^- \sim NO_3^- > F^- >> I^-$

(d) Cesium assisted Anion binding

Experimental studies on various ion-pair receptors[74,75]suggest that binding of anions are largely influenced by the presence of the cation. From table 1 and 2, it is evident that anion binding to the receptor is comparatively weaker as compared to Cs^+. Thus, cation is expected to bind first to the receptor, which can subsequently enhance the binding affinity of anion to the receptor. Here, we have considered all possible four binding modeswhich are earlier denoted as C/P, G/P, P/P and C/C (scheme 1). The cation assisted anion binding affinitiesare calculated using the following expression,

$$E_{[Receptor.Cs+]} + E_{[X-.(H2O)6]} \rightarrow E_{[Receptor.Cs+.X-]} + E_{[(H2O)6]} \quad (5)$$

For all the three available X-ray structures (CsCl, CsF and $CsNO_3$), our optimized structures are very close to the experimental data (Table 3).[25,26]For instance, the average Cs^+-O_C bond distances are within 0.1 Å deviation with respect to corresponding three X-ray structures. Notably, for $CsNO_3$ at G/P mode, in contrary to experimental observation of asymmetric binding of Cs^+ and nitrate (3.19-3.50 Å), Cs^+ is noted to interact with nitrate symmetrically (Cs^+-$O_{nitarte}$-3.26-3.28 Å). Such structural change can be attributed to the presence of crystallographic solvent molecule (ethanol) in the X-ray structure (see below).The Cs^+-O bond lengths at the 'C' site is comparatively shorter as compared to Cs^+-O_{Arene}due to strong electrostatic interactions. As expected, the X-N_p bond lengths are elongated as we go from F^- to I^- due to decreasing electronegativity which leads to weakening of hydrogen bonding down the group. Notably, Cs-O_G bond distances (G/P mode) in the complexes are found to be somewhat elongated (>0.4 Å) as compared to Cs-bound-receptor in the absence of anions. Such elongation is found to be larger as we move down the group from CsF to CsI complexes. The presence of anion at 'P' site also resulted in shortening of Cs-N_p bond distance (by ~0.1 Å in P/P mode). In contrary, the computed Cs-O_C bond distances in C/P and C/C modes remain almost unchanged with respect to [Receptor-Cs^+]. In the presence of Cs^+ at 'G' site, X-N_P bond lengths are elongated significantly (by ~0.09 Å for CsCl,~0.10 Å for CsBr, ~0.11 Å for CsI) from CsCl to CsI as compared to bare anion binding to the receptor [Receptor-X^-]. Such elongation even becomes more prominent (>0.15 Å) for the G/P mode of $CsNO_3$ complex. However, in case of CsF, X-N_P distance remain unaltered even in presence of Cs^+ at 'G' site probably due to the large inter-ionic distance between the ion-pair (~5 Å). For all salts, presence of cation at 'C' or 'P' site does not change in anion-pyrrole bond length. These observations are further suggested that the close proximity of anion near cation can induce such structural changes (specifically for G/P binding mode).

Due to the favorable columbic interaction, the presence of Cs^+ in close proximity to anions at C/C,P/P and G/P mode enhances the binding affinities of anions (table 4). Although, CsF has highest lattice energy among the Cs halides,[76] we find that the presence of Cs^+ does not appreciably enhance the binding affinity of small and high electronegative anion such as F^- at G/P mode due to larger inter ionic distance between the Cs^+ and F^-. However, for larger Br^- and I^- ion, the inter ion-pair distance decreases (~3 Å) for G/P mode which leads to significant enhancement of the binding affinity of Br^- and I^- in the presence of Cs^+(table 4). Even in the presence of Cs^+, the anion binding affinities at the C/C binding mode are noted to be weak for all Cs-salts. However, with the increasing size of halide, we find an increase in the extent of favorability for 'C' site. particularly for I^-, owing to the close inter-ionic separation at C/C binding mode (5.97 Å) and proper size compatibility between the opposite ions. Thus 'C' site is now noted to be more favorable than 'P' site in the presence Cs^+at 'C' site (Table 4). Similarly the presence of Cs^+ at 'P' site also enhances the anion binding affinities (P/P mode) by almost 6 kcal mol^{-1}.

(e) Anion assisted Cesium binding

Until now, we have shown that cationdoes assist the anion binding to the receptor. Taking consideration of binding affinity (Table 1 & Table 2), we can expect anion to bind the receptor later to Cs^+. Nevertheless, the presence of anion can also regulate cation binding ability due to the acting cooperative effect. As all the anions are noted to have unfavorable binding affinity at the outer sphere of 'C' site, hence anions are not expected to bind at the 'C' site prior to cation binding. Thus, C/C binding mode is not considered here. Anion assisted cation binding affinity is calculated using the following expression,

$$E_{[Receptor.X-]} + E_{[Cs+(H2O)6]} \rightarrow E_{[Receptor.Cs+.X-]} + E_{[(H2O)6]} \quad (6)$$

We indeed find a significant enhancement (by ~5-10 kcal mol^{-1}) of binding strength for Cs^+in the presence of anions for all modes except for CsF in G/P binding mode. As mentioned in the earlier section, particularly for the G/P mode of CsF, the larger inter ionic distance between the Cs^+ and F^- diminishes the effect of positive allosteric effect. Similar to cesium assisted anion binding, we find that proximal presence of anion in close proximity with Cs^+ (for P/P and G/P mode) assist the binding of cation most (table 4).

(f) Overall binding affinity of ion-pairs to receptor

We have also calculated the overall binding affinity for cesium salts to receptor using the following expression,

$$E_{[Receptor]} + E_{[Cs+(H2O)6]} + E_{[X-(H2O)6]} \rightarrow E_{[Rec-Cs+.X-]} + 2E_{[(H2O)6]} \quad (7)$$

As expected, the C/C binding mode is noted to be less preferable for all cesium salts except for CsI (table 5). In the

presence of I^-, the considerable preference of Cs^+ to bind at 'C' site over 'P' site in the contact ion-pair complexes of CsI (C/C and P/P) (Table 4) seems to originate slightly higher preference of C/C mode for CsI than the P/P mode. Relative binding strength of CsF in receptor is predicted to be less as compared to CsCl and CsBr. The computed binding affinity trends suggest that C/P mode to be the most favorable for CsF and CsCl, whereas $CsNO_3$ ion-pair complex prefers G/P mode which are in good correlation with experimental data.[25,26]We find that the calculated binding affinity trend for $CsNO_3$ in close agreement with experimentally observed G/P binding mode. It should be noted that with pure calix-pyrrole system which is only capable to bind ion-pair *via* P/P binding mode, Wintergerst et al.[77] reported binding of $CsNO_3$ to the host molecule is weakest (or unbound) among the three Cs salts (CsCl, CsBr and $CsNO_3$). Although our used host molecule is markedly different (as it contains 'C' site for cation) in comparison to the aforementioned calix-pyrrole system, we can qualitatively compare the performance of these two host molecules at the P/P binding site. We do predict a similar trend, where within the three salts (CsCl, CsBr and $CsNO_3$), binding affinities for $CsNO_3$ is least for the P/P binding mode (-23.59 kcal mol^{-1}- CsCl;-22.80 kcal mol^{-1}- CsBr; -20.59 kcal mol^{-1}- $CsNO_3$). Notably, for $CsNO_3$, the preference of G/P over the C/P binding site is due to the presence of favorable bi-dentate coordination between the ion pairs in the former binding motif.Particularly for large anions like Br^- and I^-, a slight preference for G/P mode over C/P mode is observed. This can be ascribed to the favorable electrostatic interactions present between the oppositely charged ions of large ionic radii at short distances which indeed help to stabilize the contact ion-pair complex formation.

(g) Role of Crystallographic solvent molecule

In the X-ray crystal structures of CsF, CsCl and $CsNO_3$ bound receptor, a crystallographic methanol molecule, a water molecule and an ethanol molecule are found(figure 2). In order to quantitatively describe the influence of these explicit solvent molecules on the structures and relative binding affinities, we further calculated the binding affinity using following expression,

$$E_{[Receptor]}+E_{[Cs+(H2O)6]}+E_{[X-(H2O)6]}+E_{[Sol]}\rightarrow E_{[Receptor.Cs+.X-.Sol]}+2E_{[(H2O)6]} \quad (8)$$

where, X= F^-, Cl^-, NO_3^- and Sol denotes CH_3OH, H_2O and C_2H_5OH

We have also calculated the relative energies (R.E in kcal mol^{-1}) for all binding modes with respect to the most stable species of all three Cs salts (table 7).

Here, we have not considered C/C binding mode as we noted this binding mode to be least favorable in previous calculations.The optimized structures (Table 6) showed very small displacement from the reported X-ray structure [RMSD: 0.357 Å (CsF), 0.309 Å (CsCl) and 0.478 Å ($CsNO_3$): see SI, Figure S2].

Although the structures are perturbed very little due to the presence of solvent molecules, the overall binding affinities are modified significantly (up to 10-15 kcal mol^{-1}, Table 7) but importantly does not alter the overall binding trends. This indeed suggests that solvent molecules in close proximity to the ions provide charge delocalization through hydrogen bonding thus stabilizing to the solvent separated Cs salt complexes.

It should be noted that a direct comparison of solvent effect on the binding affinities cannot be made between the different cesium salts due the presence of non-identical solvent molecule at different ion-pair complexes. However, we can rationalize the observed change in binding affinity with respect to different binding modes for a particular ion-pair complex.

For CsF ion-pair complex, very similar binding affinities are predicted for both C/P and G/P binding sites in the presence of a solvent methanol molecule (R.E=+1.1 kcal mol^{-1}). Here, at G/P mode, methanol acts as a bridge between the ions where hydrogen on the hydroxyl group ofthe methanol remain hydrogen bonded with F^- (1.67 Å) and oxygen of methanol coordinate to Cs^+ (2.97 Å). The inter-ionic distances are now elongated further (5.45 Å) as compared to contact ion-pair complex to form solvent bridged ion-pair complex. These subsequent changes help the ion-pair to get stabilized more inside the receptor (binding affinity increased by~15 kcal mol^{-1}). Further, we find C/P mode for CsF is slightly more favourable (by only 1 kcal mol^{-1}) as compared to G/P.This is in accord with the reported experimental observationsof Kim et al. [26]where a slow equilibrium between the G/P mode and the thermodynamically stable C/P mode was noted.However, for CsCl, the binding affinity at C/P mode still remains more preferable as compared to G/P mode but now the margin of difference is 3 kcal mol^{-1} (R.E=+3.2 kcal mol^{-1}). Similar to CsF, here also water is observed to remain hydrogen bonded albeit weakly with Cl^- (2.21 Å). Hence, an enhanced binding affinity is smaller for CsCl as compared to CsF. In case of $CsNO_3$the G/P ion-pair complexis found to be largely preferable (by 9 kcal mol^{-1}) as compared to C/P mode (R.E=+9.0 kcal mol^{-1}). Here, Cs^+ interacts strongly with the oxygens of the 'G'site (figure 2). As mentioned earlier, an asymmetric strong bi-dentate interaction of NO_3^- with Cs^+ (3.34-3.59 Å) is also noticed resulting in a strongly favourable binding as compared to P/P and C/P modes. For $CsNO_3$ binding at G/P site, Cs^+ interact with an oxygen atom of an ethanol molecule (3.19 Å) while a strong hydrogen bonding interaction with ethanol and NO_3^- (1.92 Å) further stabilize the structure leading to very strong binding affinity through a solvent bridged ion pair complex thus the overall binding affinity is stabilized by ~10 kcal mol^{-1}.

(h) Comparison with reported MM calculations

Contrary to previously reported gas phase MM calculations[25, 26] (Table 7), our calculations predict favourable binding modes more accurately. Although the experimental X-ray and NMR data favor C/P binding mode for CsF, CsCl and G/P mode for $CsNO_3$, the MM calculations conclude favorability of G/P binding motif for both CsF, CsCl. However, for $CsNO_3$ the MM calculations do predict the correct G/P binding mode to be most preferable. Notably, unlike MM calculations, the present computational methodology incorporates the implicit solvent effect through the COSMO solvation model. To understand whether the incorrect trend predicted by MM calculations originates due to solvation, we further calculated the binding affinities of CsCl with the receptor in the gas phase (table 8). We note that absolute binding affinities are larger as compared to the solvated systems. More importantly, here also gas phase calculations failed to follow the experimental trend. Hence, owing to the lack of solvation effects,

incorrect binding affinity trends were predicted.

Finally, to gauge the influence of different solvent media to the binding affinities, calculations with [Receptor.CsCl] were performed with chloroform as solvent (ε=5.5). The net binding affinity of all the complexes increases by almost 8-15 kcal mol^{-1}but overall the favourability towards C/P binding mode remain unchanged at both solvent environments (ref SI, Table S4). This provides further support to the notion that solvent media of low polarity can modulate the extraction efficiency of Cs salts to the receptor.

(i) Energy Decomposition Analysis (EDA)

The nature of the interactions present between the radionuclides and the receptor has been further analysed through EDA (table 9). It is well known that the total interaction energy of a complex strongly varies with the use of different fragment systems. With view of this, here we have considered two different fragment pairs viz. FP_A and FP_B. FP_A investigates the interactions between cesium bound receptor with anions, whereas fragment FP_B deals with the interaction between anion bound receptor with cesiumcation. EDA calculations have been performed for the most preferred binding mode of CsX complexes (i.e. C/P mode for CsF,CsCland G/P mode for CsBr, CsI and $CsNO_3$).

For both the fragment pairs i.e. $FP_A$and FP_B, we find the contribution of electrostatic interaction ($\Delta \boldsymbol{E}_{\mathbf{elstat}}$) is considerably higher (>70 %) as compared to orbital interaction ($\Delta \boldsymbol{E}_{\mathbf{orb}}$) (~20-30 %) in the overall interaction energy. This is suggestive of the fact that the electrostatic interaction of cesium and anion at their corresponding binding site plays a dominant role in stability of the complex. This is also revealed in the QTAIM study (see below). Further, for all complexes, negative value of total interaction energy points towards the well stabilization of cesium and anion inside the complex. In case of FP_A, The bonding energy is noted to be more negative for the [Receptor.Cs^+]$\cdots$[F^-] than the other anions. The $\Delta \boldsymbol{E}_{\mathbf{orb}}$ is significantly more negative for the [Receptor.Cs^+]$\cdots$[F^-] than [Receptor.Cs^+]$\cdots$[Cl^-], resulting in the greater stability of the former by 22 kcal mol^{-1}. In addition, the total steric interaction is less attractive in [Receptor.Cs^+]$\cdots$[Cl^-] than the others due to the lesser contribution from electrostatic interaction term to this pair. The Pauli repulsion for the cesium bound receptor and anion is lower for all other anions as compared to F^-. For FP_B, The total steric interaction is estimated to be more negative for Br^-, I^- and NO_3^- bound receptor due to the lesser contribution of Pauli repulsion term.

(j) QTAIM Analysis

We have investigated the topological properties at the BCPs forthe most favourable receptor-Cs^+X^- complexes (refer SI, table S5-S9). All the systems analyzed here clearly display BCPs indicating the non-bonded interactions that exist between the Cs^+/X^- and receptor molecule. In the molecular graph, the big circles correspond to attractors attributed to positions of atoms and critical points such as (3, -1) BCP (red), (3, +1) RCP (yellow) and (3, +3) CCP (green) indicated by small circles (refer SI, figure S4).

In the C/P-CsF complex, seven different bond paths have been observed between F^- and 'P' site. Of the seven bond paths, four are N-H$\cdots$F type and remaining three are C-H$\cdots$F type interactions (refer SI, figure S3). Of the three C-H$\cdots$F interactions, two corresponds to the hydrogen bonding between the methine hydrogens of the 'P' site and the anions, whereas the last one is attributed to the hydrogen bonding of anions with nearby hydrogen of calix[4]arene moiety. C/P-CsCl system also noted to have these seven different bond paths and additionally two $C_\pi\cdots$Cl interactions are also observed (Figure 3). The calculated topological properties at the BCP between the interacting atoms with the corresponding anions suggest that as the size of the anions increases, the charge density at BCP decreases. For a typical hydrogen bond, the values of the electron density at the BCP should be within 0.002–0.035 a.u.[78] Our calculated value for the anions bound in 'P' site falls in this range (refer SI, table S5-S9). It is interesting to note that, mainly H$\cdots$X bonding interactions stabilize the incoming anions. The ρ values at the H$\cdots$X BCPs suggest that there are seven such hydrogen bonding interactions that fall into two distinct sets. Among the seven hydrogen bonds, four are comparatively stronger whose ρ values lie at ~ 0.0165 a.u. whereas for the remaining three weak hydrogen bonds, this value lies at ~0.003 a.u. These varying degrees are consistent with the geometric parameters (table 3). It is clear that the hydrogen bonding between the methine hydrogens of the 'P' site and the anions ions are not symmetric and the strength of the hydrogen bonds is distinguished using the properties of the electron density at BCP. It is interesting to find that the four strong hydrogen bonds (N-H$\cdots$X) get weakened and other three weak hydrogen bonds (C-H$\cdots$X) are strengthened gradually as we move from the fluoride to iodide. Interestingly, in the $CsNO_3$ ion-pair complex, NO_3^- shows different bond paths between the NO_3^- anion and 'P' site and with the aromatic linker.

Cremer and Karaka[79] have developed a scale to determine the nature of bonds based on these topological properties. Accordingly, in all the cases the BCPs between C-H$\cdots$X bonds have negative Laplacian, a positive kinetic energy density H(r) and a potential energy to the lagrangian kinetic energy ratio (|V(r)/G(r))| of less than 1. Critical points with such characteristics have been identified by Cremer as constituted by atoms that share a shared interaction (ionic, van der Waals, or hydrogen bonds). While the negative L(r) values and small negative H(r) values along with a –|V(r) /G(r)| values at the BCPs between N-H$\cdots$X bonds are indicative of a weak non-bonding interactions. As it is obvious from Table S5-S9, the ellipticity values (ε) for the N–H$\cdots$X and C-H$\cdots$X interactions are nearly small and close to zero, indicating that the hydrogen bonds are conserved in all the complexes. For Cs^+ at the 'C' site the small values of ρ, the high values of ε and the nearly zero values of H(r) suggest, according to the Rozas[80] criterion, that all Cs$\cdots$O intermolecular interactions, are basically electrostatic in nature (Figure 3). More specifically, it can be seen that the values of ellipticity obtained for the Cs$\cdots$O interactions are within the

range of 0.072–1.133. The existence of Cπ···Cs^+ interactions is also revealed by the presence of corresponding BCPs in the molecular graphs (refer SI, figure S4). In 'G' site, bond paths have been observed between the Cs^+ and aromatic moieties of calix-4-arene along with the ethylene glycol spacer interactions.

Conclusions

An increasing interest and urgency is devoted to improve the nuclear waste management processes through the design of new receptor macrocycles. Sessler and co-workers have designed a series of macrocycles for the selective extraction of Cs^+. Various mechanisms for the binding of Cs salt to the receptor have been suggested. In this manuscript, we have carried out a systematic study to understand the structure, binding and selectivity of various Cs salts to a recently synthesized receptor[25,26]using electronic structure calculations. To our knowledge, the electronic structure calculations reported here are the first to be carried out on such gigantic receptor without truncations. The major findings from our study are summarized as follows:

(i) We find that Cs^+ alone can favorably bind to 'C' and 'G' site of the receptor. The binding of anions occurs at the 'P' site, preferably due to the strong hydrogen bonding between the protons of the pyrrole ring and the anions.

(ii) Computed binding affinities further indicate that the ion-pair binding to the receptor occurs majorly *via* cooperative binding mechanism. Both Cs^+ and anion assist each other to provide excess stability to the ion-pair receptor complex.

(iii) In accord to experiments, we find C/P mode to be most preferable for CsF and CsCl while G/P for $CsNO_3$. The presence of a crystallographic solvent molecule is also observed to enhance the overall binding affinity of the Cs salt to the receptor by 1-15 kcal mol^{-1}.

(iv) Irrespective of fragment pair (A and B), electrostatic contribution ($\Delta \boldsymbol{E}_{\mathbf{elstat}}$**)** to the total interaction energy is estimated to be higher than the orbital interaction ($\Delta \boldsymbol{E}_{\mathbf{orb}}$**).** QTAIM calculations clearly bring out the importance of strong hydrogen bonding interactionswhich stabilizes the anions at the 'P' site. In line with our EDA results, QTAIM also reveals the bonding of Cs^+ at 'C' and 'G' site is dominantly ionic in nature. Further, our results demonstrate the bulk solvent effects are crucial for the correct binding trends of Cs salts to the receptor. Thus, the applied theoretical tools can be used to predictand design new receptor molecules for the complexation of various other radionuclides such as Sr^{2+}. Future work on this direction is ongoing in our computational laboratory.

Acknowledgements

MS thanks Dr. B. N. Jagatap for his kind support and the BARC computer center for providing the high performance parallel computing facility (Adhya and Ajeya Systems). BS thanks Dr.Tusar Bandyopadhyay, Shri. R. Singh, Dr. K.S. Pradeepkumar for their continuous support and encouragement. P.V thanks Council of Scientific and Industrial Research (CSIR) for the award of an Emeritus Scientistship (Award Letter No. 21(0936)/12/EMR-II) and Department of Science & Technology (DST), India for Major Research Project (Ref. No: SB/S1/PC-52/2012).

References

1. D. C. Adriano, G. D. Hoyt and J. E. Pinder, *Health Phys.,*1981**, 40**, 369.
2. H.Carlton, L. R. Bauer, A. B. Evans, L. A. Beary, C.E. Murphy, J. E. Jr. Pinder, and. R. N. Strom, WSRC-RP, Aiken, SC.1992, 92.
3. V. N. Egorov, P. P. Povinec, G. G. Polikarpov, N. A. Stokozov, S. B. Gulin, L. G. Kulebakina and I. Osvath, *J. Environ. Radioact.,* 1999, **43**, 137.
4. K.V. Ticknor, and Y.H. Cho, *J. Radioanal. Nucl.Ch*., 1990, **140**, 75.
5. J. Handl, *Radiochim. Acta*, 1996, **72**, 33.
6. A. Aarkrog, *J. Environ. Radioact.***,**1988**, 6***,* 151.
7. A. Stohl, P. Seibert, G. Wotawa, D. Arnold, J. F. Burkhart,; S. Eckhardt,; C. Tapia, A. Vargas and T. J.Yasunari, *Atmos. Chem. Phys. Discuss*., 2011, **11**, 28319.
8. S. Maleknia and J. Brodbelt, *J. Am. Chem.Soc.*1992, **114**,4295.
9. C. Bocchi, M. Careri, A. Casnati and G. Mori, *Anal. Chem*, 1995, **67,** 4234.
10. Ji, H. F, Dabestani, R, Brown, G. M, and Sachleben, R. A, *Chem. Commun.*, 2000, **10**, 833.
11. A. Casnati, A. Pochini, R. Ungaro, J. F. Ugozzoli, F. Arnaud, S. Fanni, M. J. Schwing, Richard, J. M. Egberink, F. de Jong and D. N. Reinhoudt, *J. Am. Chem. Soc*. 1995, **117**, 2767.
12. E. Ghidini, F. Ugozzoli, R. Ungaro, S. Harkema, A. A. El-Fadl and D. N. Reinhoudt, *J. Am. Chem. Soc.* 1990, **112**, 6979.
13. Asfari, Z, Bressot, C, Vicens, J, Hill, C, Dozol, J. F, Rouquette, H, andTournois, B,*Analytical Chemistry*, 1995, **67**, 3133.
14. S. Chakraborty, R. Dutta, B. M. Wong and P. Ghosh, *RSC Advances,* 2014, **4**, 62689.
15. S. Chakraborty, R. Dutta, M. Arunachalam and P. Ghosh, *Dalton Trans.,* 2014, **43**, 2061.
16. P. A. Gale, J. L. Sessler and V. Kral, *Chem. Commun*., 1998, 1.
17. P. A. Gale, M.B. Hursthouse, M. Light, J. L. Sessler, A .N. Warriner and R. S. Zimmerman, *Tetrahedron Letters,* 2001*,* **42**, 6759.
18. B. Turner, A. Shterenberg, M. Kapon, K. Suwinska and Y. Eichen, *Chem. Commun.*, 2001, 13.
19. R. Custelcean, L. H. Delmau, B. A. Moyer, J. L. Sessler, W. S. Cho, D. Gross and , P. A. Gale, *Angew.Chim. Intl. Ed.*, 2005, **117**, 2593.
20. H. Miyaji, W. Sato and J. L. Sessler, *Angew.Chem.,* 2000**,112**, 1847.
21. P. Anzenbacher, A. C. Try, H. Miyaji, K. Jursı´kova´,V.M. Lynch, M. Marquez and J. L. Sessler, *J. Am. Chem. Soc.* 2000, **122**, 10268.
22. J. L. Sessler, D.E. Gross, W. Cho, V. M. Lynch, F. P. Schmidtchen, G.W. Bates, M. E. Light and P. A. Gale, *J. Am. Chem. Soc.*, 2006, **128**, 12281.

23. S. K. Kim, J. L. Sessler, D. E. Gross, C. Lee, J. S. Kim, V. M. Lynch, L. H. Delmau and B. P. Hay. *J. Am. Chem. Soc.*, 2010, **132**, 5827.

24. J. L. Sessler, S. K. Kim, D. E. Gross, C. Lee, J. S. Kim and V. M. Lynch,*J. Am. Chem. Soc.*, 2008, **130**, 13162.

25. S. K. Kim, G. I. Vargas-Zuniga, B. P. Hay, N. J. Young, L. H. Delmau, C. Masselin, C. Lee, J. S. Kim, V. M. Lynch, B. A. Moyer and J. L. Sessler, *J. Am. Chem. Soc.,* 2012, **134,** 1782.

26. S. K. Kim, V. M. Lynch, N. J. Young, B. P. Hay, C. H. Lee, J. S. Kim and J. L. Sessler, *J. Am. Chem. Soc.*, 2012, **134**, 20837.

27. A. Boda and M. A. Sheikh, *J. Phys. Chem.A*, 2012, **116**, 8615.

28. S.E. Hill, D. Feller and E. D. Glendening, *J. Phys. Chem.A*, 1998, **102**, 3813.

29. M. Sundararajan, R. V. Solomon, S. K. Ghosh and P. Venuvanalingam, *RSC Adv.* 2011, **1**, 1333.

30. J. Kriz, J. Dybal, E. Makrlik and Z. Sedlakova, *Chemical Physics*, 2012, **400**, 19.

31. C. D. Kumar, B. Sharma, Y. Soujanya, V. N. Chary, S. R. Patpi, S. Kantevari, G .N. Sastry and S. Prabhakar, *Phys. Chem. Chem. Phys.,* 2014, **16**, 17266.

32. J. Narbutt, A. Wodynski, M. Pecul, *Dalton Trans.,* 2015, **44**, 2657.

33. A. D. Becke, *Phys. Rev. A,* 1988, **38**, 3098.

34. J. P. Perdew, *Phys. Rev. B,* 1986, **33**, 8822.

35. A. Schäfer, H. Horn and R. Ahlrichs, *J. Chem. Phys.,* 1992, **97**, 2571.

36. P. K. Verma, P. N. Pathak, N. Kumari, B. Sadhu, M. Sundararajan, V. K. Aswal and P. K. Mohapatra, *J. Phys. Chem. B*., 2014, **118**, 14388.

37. P. K. Verma, N. Kumari, P. N. Pathak, B. Sadhu, M. Sundararajan, V. K. Aswal, P. K. Mohapatra, *J. Phys. Chem. A*., 2014, **118**, 3996.

38. M. Sundararajan, V. Sinha, T. Bandyopadhyay and S. K. Ghosh, *J. Phys. Chem. A.* 2012, **116**, 4388.

39.P. K. Verma, P. N. Pathak, P. K. Mohapatra, V. K. Aswal, B. Sadhu, M. Sundararajan, *J. Phys. Chem. B*.. 2013, **117**, 9821.

40. A. Klamt, and G. Schüürmann, *J. Chem. Soc, Perkin Trans. 2*, **1993**, 799.

41. A. Schäfer, C. Huber and R. Ahlrichs, *J. Chem. Phys.,* 1994, **100**, 5829.

42. F. Weigend and R. Ahlrichs, *Phys. Chem. Chem. Phys*., 2005, **7**, 3297.

43. S. Grimme, J. Antony, S. Ehrlich and H. Krieg, *J. Chem. Phys.* 2010, **132**, 154104.

44. A. D. Becke, *J. Chem. Phys.,* 1993, **98**, 5648.

45. C. Lee, W. Yang and R.G. Parr, *Phys. Rev. B*, 1988, **37**, 785.

46. J. P. Austin, M. Sundararajan, M. A. Vincent, and I. H. Hillier, 2009, *Dalton Trans.*, **30**, 5902.

47. P. Wåhlin, C. Danilo, V. Vallet, F. Réal, J. P. Flament, and U. Wahlgren, 2008, *J. Chem. Theory Comput*, **4**, 569.

48. T. Leininger, A. Nicklass, W. Kuechle, H. Stoll, M. Dolg and A. Bergner, *Chem. Phys. Lett*. 1996, **255**, 274.

49. J. L. Whitten, *J. Chem. Phys.,* 1973, **58**, 4496.

50. E. J. Baerends, D. E. Ellis and P. Ros, *Chem. Phys.,* 1973, **2**, 41.

51. B.I. Dunlap, J.W.D. Connolly and J. R. Sabin, *J. Chem.Phys.,* 1979, **71**, 3396.

52. C. Van Alsenoy, *J. Comp. Chem.,* 1988, **9**, 620.

53. K. Eichkorn, O. Treutler, H. Öhm, M. Häser and R. Ahlrichs, *Chem. Phys. Letters.* 1995, **240**, 283.

54. M. Sundararajan, *J. Phys. Chem. B*, 2013, **117**, 13409.

55. B. Sadhu, , M. Sundararajan and T.Bandyopadhyay, 2015. *J. Phys. Chem. B.* ASAP.

56. R. Ahlrichs, M. Bar, H.-P. Baron, R. Bauernschmitt, S. Bocker, M. Ehrig, K. Eichkorn, S. Elliot, F. Furche, F. Haase, M. Haser, H. Horn, C. Huber, U. Huniar, M. Kattannek, C. Kolmel, M. Koolwitz, K. May, C. Ochsenfeld, H. Ohm, A. Schafer, U. Schneider, O. Treutler, M. von Arnim, F. Weigend, P. Weis and H. Weiss, TURBOMOLE V6.3.1 2011, a development ofUniversity of Karlsruhe and Forschungszentrum Karlsruhe GmbH, 1989-2007, TURBOMOLE GmbH, since 2007; available from http://www.turbomole.com.

57. F. Neese, ORCA Version 3.0, Ab initio density functional and semiempirical program package, 2013.

58. G. teVelve, F. M.Bickelhaupt, E. J.Baerends, van S. J. A.Gisbergen, C.Fonseca Guerra, J. G.Snijders, T.Ziegler, *J. Comput. Chem.* 2001, **22,**931.

59. K. Morokuma, *J. Chem. Phys.,*1971, **55**, 1236.

60. T. Ziegler, A.Rauk, *Theor. Chim.Acta,* 1977, **46**, 1.

61. J. Xie, W. Feng, P. Lu and Y. Meng, *Computat. Theoret. Chem.*, 2013, **1007**, 1

62. D. B. Pardue, S. J. Gustafson, R. A. Periana, D. H. Ess, and T. R. Cundari, *Computat. Theoret. Chem.* 2013, **1019**, 85.

63. R. F. W. Bader, Oxford University Press, Oxford, UK, 1990, vol. 2.

64. R. F. Bader, *J. Phys. Chem. Rev.A*, 2009, **113**, 10391.

65. K. K. Pandey, P. Patidar, P. K. Bariya, S. K. Patidar, andR. Vishwakarma, *Dalton Trans.*, 2014, **43**, 9955.

66. F. Biegler-König and J. Schönbohm, *J. Comput. Chem.,* 2002, **23**, 1489.

67. I. A. Topol, G. J. Tawa, S. K. Burt and A. A. Rashin, *J. Chem. Phys.,* 1999, **111**, 10998.

68.L. X. Dang and B. C. Garrett, *J. Chem. Phys.,* 1993, **99**, 2972.

69. S. M. Ali, S. De and D. K. Maity, *J. Chem. Phys.,* 2007, **127**, 044303.

70. Y. Marcus, *J. Chem. Soc., Faraday Trans.*, 1991, **87**, 2995.

71. F. Pichierri, *J. Mol. Struc-Theochem.,* 2002, **581**, 117.

72. Y. Wu, D. Wang and J. L. Sessler, *J. Org. Chem.* 2001, **66**, 3739.

73. T. Steiner, *ActaCryst. B*, 1998, **54**, 456.

74. I.-W. Park, J.Yoo, B. Kim, S. Adhikari, S. K. Kim, Y. Yeon, C. J. E. Haynes, J. L. Sutton, C. C. Tong, V. M. Lynch, J. L. Sessler and P. A. Gale, *Chem. Eur. J.,* 2012, **18**, 2514.

75. J. L. Sessler, S. K. Kim, D. E. Gross, C. -H. Lee, J. S. Kim, V. M. Lynch, *J. Am. Chem. Soc.* 2008, **130**, 13162.

76. Gopikrishnan, C. R, Jose, D, and Datta, A, *AIP Advances*, 2012,**2**, 012131.

77. M. P. Wintergerst, T. G. Levitskaia, B. A. Moyer, J. L. Sessler and L. H. Delmau, *J. Am. Chem. Soc.,*2008, **130,** 4129.

78. C. F. Matta, N. Castillo and R. J. Boyd, *J. Phys. Chem.A,* 2005, **10**, 93669.

79. D. Cremer and E. Kraka, *Croat. Chem. Acta*, 1984, **57**, 1259.

80. I. Rozas, I. Alkorta, Elguero, *J. Am. Chem. Soc.,* 2000, **122**, 11154.

Table Captions

Table 1. Calculated Cs^+ binding and relative affinities (B.E and R. E, in kcal mol^{-1}) to the receptor.

Table 2. Calculated anion binding affinities (B. E units in kcal mol^{-1}) to the receptor.

Table 3.Optimized structural parameters (Å) of Receptor-Cs^+X^- complex.

Table 4. Cs^+ assisted anion (X^-) and anion (X^-) assisted Cs^+ binding affinity (B. E, units in kcal mol^{-1}) to receptor.

Table 5. Net Cs^+X^- binding affinity (B. E, units in kcal mol^{-1}) to the receptor

Table 6. Optimized structural parameters (Å) of Receptor-Cs^+X^- complex in presence of solvent molecule

Table 7. Calculated binding affinities (B. E, units in kcal mol^{-1}) and relative energies (R. E, units in kcal mol^{-1}) of [Receptor.CsX] (X= F^-, Cl^-, NO_3^-) complex in the presence of crystallographic solvent molecule.

Table 8. Gas phase binding affinities (B. E, units in kcal mol^{-1}) of CsCl in receptor at B3LYP-D3/B2//BP86/B1 level

Table 9. Energy decomposition analysis (energies in kcal mol^{-1}) on complexes of Cesium Salts with Receptor at BLYP/TZ2P level. The values in the parentheses give the percentage contribution to the total attractive interactions ($\Delta E_{\text{Elstat}} + \Delta E_{\text{Orb}}$).

Figure Captions

Scheme 1: Possible binding modes of Cs^+X^- in Receptor.

Figure 1. Structure of ion-pair receptor

Figure 2. Optimized structures of (a) Receptor-Cs^+F^-complex (C/P binding mode), (b) Receptor-Cs^+Cl^- complex (C/P binding mode) and (c) Receptor-$Cs^+NO_3^-$ complex (G/P binding mode) in the absence and presence of solvent molecule. Primary interactions are shown using ball and stick model.

Figure 3. The Laplacian of electron density describing the (a) C-H···Cl interaction (calix[4]pyrrole) (b) C-H···Cl interaction (calix[4]arene) (c) C-H···Cl interaction (π-spacer) (d) (a) $Cs^{\cdots}O_C$ interaction of Receptor-Cs^+Cl^- complex (C/P).

Scheme 1: Possible binding modes of $Cs^{+}X^{-}$ in Receptor.

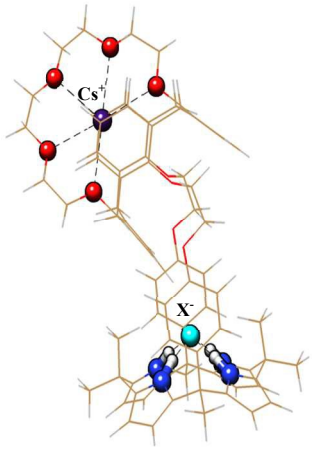	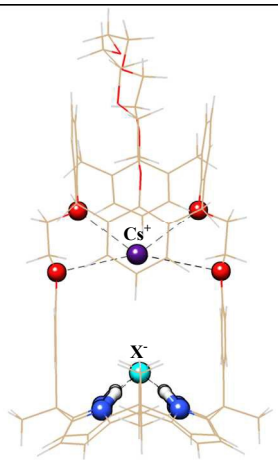	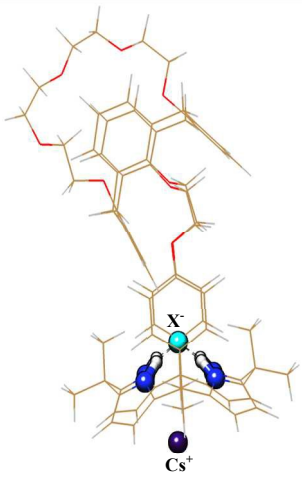	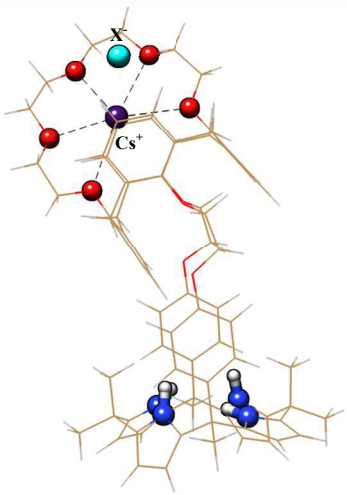
Crown/Pyrrole (C/P)	**Glycol/Pyrrole (G/P)**	**Pyrrole/Pyrrole (P/P)**	**Crown/Crown (C/C)**

Table 1. Calculated Cs^+ binding and relative affinities (B.E and R. E, in kcal mol^{-1}) to the receptor.

Cation	Binding site	R.E	B. E
Cs^+	Crown 'C'	0	-15.11
	Glycol 'G'	+2.06	-13.05
	Pyrrole 'P'	+8.35	-6.76

Table 2. Calculated anion binding affinities (B. E units in kcal mol^{-1}) to the receptor.

Anions	'P' site	'C' site
F^-	-5.64	+30.96
Cl^-	-8.44	+11.36
Br^-	-8.21	+5.52
I^-	+1.72	+7.96
NO_3^-	-7.57	+6.06

Table 3.Optimized structural parameters (Å) of Receptor-Cs^+X^- complex.[a]

	$Cs\text{-}O_{C/G}$	$Cs\text{-}C_A$[b]	$Cs\text{-}N_P$	$X\text{-}N_P$
Receptor-Cs^+.F^-				
G/P	3.15-3.99	3.48-3.55	-	2.72-2.73
C/P	2.90-3.10 (2.84-3.03)	3.40-3.43(3.40-3.46)	-	2.72-2.73 (2.76-2.81)
C/C	2.97-3.19	3.41-3.62	-	-
P/P	-	-	3.47-3.52	2.72-2.73
Receptor-Cs^+.Cl^-				
G/P	3.34-4.08	3.44-3.67	-	3.29-3.30
C/P	2.94-3.12(2.84-3.10)	3.44-3.45 (3.29-3.40)	-	3.21-3.23 (3.23-3.31)
C/C	2.98-3.10	3.39-3.83	-	-
P/P	-	-	3.53-3.55	3.21-3.22
Receptor-Cs^+.Br^-				
G/P	3.30-4.13	3.45-3.61	-	3.48-3.51
C/P	2.92-3.10	3.45-3.46	-	3.40-4.42
C/C	2.99-3.13	3.41-3.73	-	-
P/P	-	-	3.55-3.57	3.38-3.40
Receptor-Cs^+.I^-				
G/P	3.17-4.21	3.49-3.58	-	3.71-3.76
C/P	2.92-3.11	3.45-3.52	-	3.60-3.66
C/C	2.92-3.10	3.45-3.52	-	-
P/P	-	-	3.56-3.57	3.61-3.66
Receptor-Cs^+.NO_3^-				
G/P	3.23-3.62 (3.01-3.63)	3.48-3.67 (3.48-3.76)	-	2.93-2.97 (2.92-3.00)
C/P	2.93-3.11	3.38-3.51	-	2.79-2.85
C/C	2.94-3.15	3.42.3.43	-	-
P/P	-	-	3.56-3.59	2.83-2.89

[a] Values in parenthesis are the corresponding experimental values (ref no.25, 26).

[b]Cs^+-C_A refer to the distance between Cs^+ and ortho and meta carbon atoms of Calix[4]arene moiety with respect to the phenoxy groups.

Table 4. Cs^+ assisted anion (X^-) and anion (X^-) assisted Cs^+ binding affinity (B. E, units in kcal mol^{-1}) to receptor.

Binding Mode	Cs^+ assisted X^- binding[a]					X^- assisted Cs^+ binding[b]				
	F^-	Cl^-	Br^-	I^-	NO_3^-	F^-	Cl^-	Br^-	I^-	NO_3^-
G/P	-4.27 (-5.64)	-14.76 (-8.44)	-15.81 (-8.21)	-6.24 (+1.72)	-21.63 (-7.57)	-11.69 (-13.05)	-19.37 (-13.05)	-20.65 (-13.05)	-21.02 (-13.05)	-27.11 (-13.05)
C/P	-7.61 (-5.64)	-13.55 (-8.44)	-12.71 (-8.21)	-2.25 (+1.72)	-12.63 (-7.57)	-17.08 (-15.11)	-20.23 (-15.11)	-19.62 (-15.11)	-19.09 (-15.11)	-20.17 (-15.11)
C/C	+23.45 (+30.96)	+3.12 (+11.36)	-2.85 (+5.52)	-2.58 (+7.96)	+1.08 (+6.06)	-	-	-	-	-
P/P	-11.64 (-5.64)	-16.83 (-8.44)	-16.04 (-8.21)	-5.13 (+1.72)	-13.82 (-7.57)	-12.77 (-6.76)	-15.15 (-6.76)	-14.59 (-6.76)	-13.61 (-6.76)	-13.01 (-6.76)

[a] Values in parenthesis denote for anion binding affinity in the absence of the cation.
[b] Values in parenthesis denote for cation binding affinity in the absence of the anion

Table 5. Net Cs^+X^- binding affinity (B. E, units in kcal mol^{-1}) to the receptor

Binding Mode	Cs^+F^-	Cs^+Cl^-	Cs^+Br^-	Cs^+I^-	$Cs^+NO_3^-$
G/P	-17.32	-27.82	-28.86	-19.30	-34.68
C/P	-22.72	-28.67	-27.83	-17.37	-27.74
C/C	+8.34	-11.99	-17.96	-12.54	-14.03
P/P	-18.40	-23.59	-22.80	-11.89	-20.59

Table 6. Optimized structural parameters (Å) of Receptor-Cs^+X^- complex in presence of solvent molecule[a]

	$Cs\text{-}O_{C/G}$	$Cs\text{-}C_A$[b]	$Cs\text{-}N_P$	$X\text{-}N_P$
Receptor-$Cs^+.F^-.CH_3OH$				
G/P	3.14-3.85	3.48-3.80	-	2.77-2.80
C/P	2.93-3.11 (2.84-3.03)	3.47-3.51 (3.40-3.46)	-	2.72-2.76 (2.76-2.81)
P/P	-	-	3.51-3.56	2.72-2.75
Receptor-$Cs^+.Cl^-.H_2O$				
G/P	3.10-4.47	3.39-3.55	-	3.25-3.27
C/P	2.92-3.11 (2.84-3.10)	3.45-3.51 (3.29-3.40)	-	3.23-3.26 (3.23-3.31)
P/P	-	-	3.53-3.58	3.24-3.29
Receptor-$Cs^+.NO_3^-.C_2H_5OH$				
G/P	3.17-3.68 (3.01-3.63)	3.53-3.93 (3.48-3.76)		2.93-2.94 (2.92-3.00)
C/P	2.93-3.11	3.46-3.54	-	2.87-2.92
P/P	-	-	3.54-3.59	2.82-2.92

[a] Values in parenthesis are the corresponding experimental values (ref no.25, 26)

[b] $Cs^+\text{-}C_A$ refer to the distance between Cs^+ and ortho and meta carbon atoms of Calix[4]arene moiety with respect to the phenoxy groups.

Table 7. Calculated binding affinities (B. E, units in kcal mol^{-1}) and relative energies (R. E, units in kcal mol^{-1}) of [Receptor.CsX] (X= F^-, Cl^-, NO_3^-) complex in the presence of crystallographic solvent molecule.[a]

Binding Mode	Net BE for CsF	MM prediction[26]	R.E	Net BE for CsCl	MM prediction[25]	R.E	Net BE for $CsNO_3^-$	MM prediction[25]	R.E
G/P	-32.26 (-17.32)	-193.1	+1.1	-29.45 (-27.82)	-135.5	+3.2	-44.46 (-34.68)	-135.8	-
C/P	-33.32 (-22.72)	-165.6	-	-32.62 (-28.67)	-115.8	-	-35.47 (-14.03)	-116.7	+9.0
P/P	-18.08 (-18.40)	-182.5	+15.2	-29.57 (-23.59)	-117.6	+3.0	-26.88 (-20.59)	-103.5	+17.6

[a] Values in parenthesis denote for binding affinity without the influence of crystallographic solvent molecule

Table 8. Gas phase binding affinities (B. E, units in kcal mol^{-1}) of CsCl in receptor at B3LYP-D3/B2//BP86/B1 level

Binding Mode	Binding energy
G/P	-105.04
C/P	-90.22
C/C	-80.88
P/P	-105.04

Table 9. Energy decomposition analysis (energies in kcal mol^{-1}) on complexes of Cesium Salts with Receptor at BLYP/TZ2P level. The values in the parentheses give the percentage contribution to the total attractive interactions ($\Delta E_{Elstat} + \Delta E_{Orb}$).

Fragment Pair	Complex	Binding Mode	Pauli repulsion ΔE_{pauli}	Electrostatic interaction ΔE_{elstat}	Total steric interaction	Orbital interactions ΔE_{orb}	Total interaction energy ΔE_{int}
FP_A	Receptor-$Cs^{+}\cdots F^{-}$	C/P	81.04	-142.31 (70.78)	-61.27	-58.73 (29.22)	-120.00
	Receptor-$Cs^{+}\cdots Cl^{-}$	C/P	68.68	-105.93 (74.54)	-37.25	-36.18 (25.46)	-73.43
	Receptor-$Cs^{+}\cdots Br^{-}$	G/P	56.42	-115.25 (81.69)	-58.83	-25.84 (18.31)	-84.67
	Receptor-$Cs^{+}\cdots I^{-}$	G/P	64.34	-112.90 (83.06)	-48.52	-23.03 (16.94)	-71.59
	Receptor-$Cs^{+}\cdots NO_3^{-}$	G/P	55.51	-117.50 (80.46)	-62.00	-28.54 (19.54)	-90.53
FP_B	Receptor-$F^{-}\cdots Cs^{+}$	C/P	55.28	-87.81 (72.03)	-32.52	-34.09 (27.97)	-66.62
	Receptor-$Cl^{-}\cdots Cs^{+}$	C/P	51.58	-84.86 (71.85)	-33.27	-33.24 (28.15)	-66.52
	Receptor-$Br^{-}\cdots Cs^{+}$	G/P	20.13	-74.46 (74.33)	-54.33	-25.71 (25.67)	-80.04
	Receptor-$I^{-}\cdots Cs^{+}$	G/P	25.58	-77.94 (73.20)	-52.36	-28.54 (26.80)	-80.90
	Receptor-$NO_3^{-}\cdots Cs^{+}$	G/P	25.66	-85.50 (74.22)	-59.83	-29.70 (25.78)	-89.54

Figure 1. Structure of ion-pair receptor

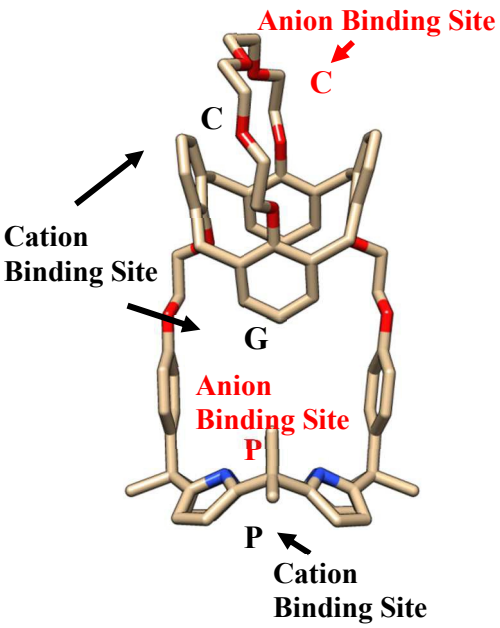

Figure 2. Optimized structures of (a) Receptor-Cs^+F^-complex (C/P binding mode), (b) Receptor-Cs^+Cl^- complex (C/P binding mode) and (c) Receptor-$Cs^+NO_3^-$ complex (G/P binding mode)in the absence and presence of solvent molecule. Primary interactions are shown using ball and stick model.

(a)

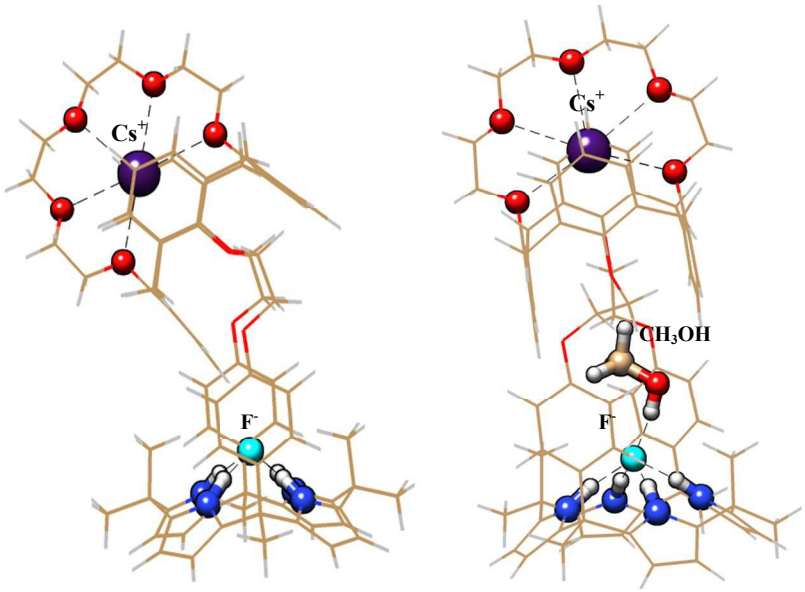

Receptor-Cs^+F^- Receptor-$Cs^+F^-.CH_3OH$

(b)

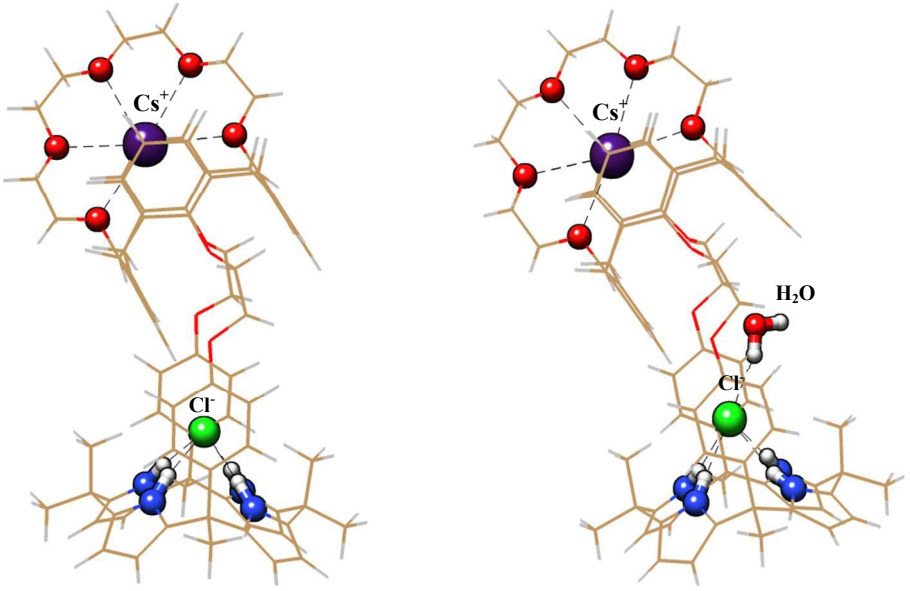

Receptor-Cs^+Cl^- Receptor-$Cs^+Cl^-.H_2O$

(c)

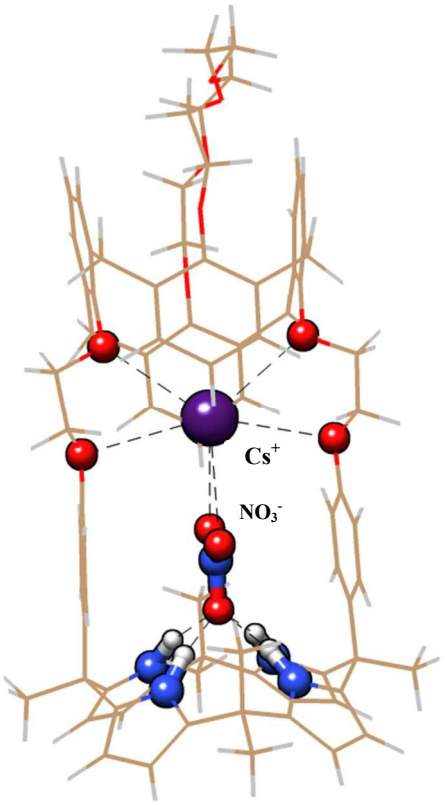

Receptor-$Cs^{+}NO_3^{-}$

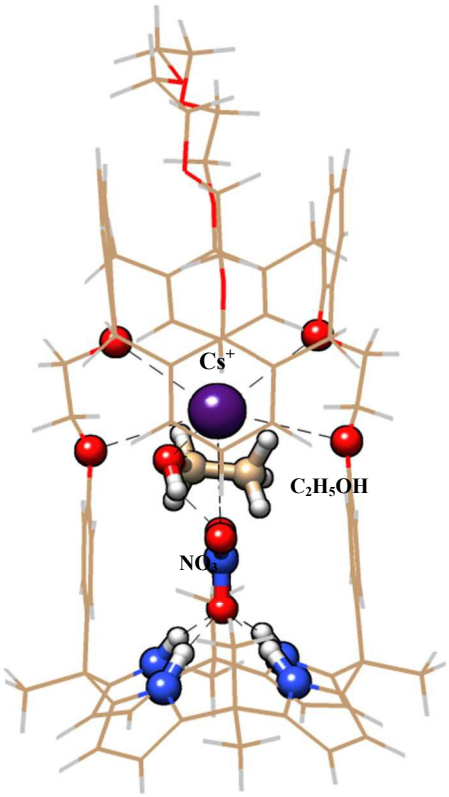

Receptor-$Cs^{+}NO_3^{-}.C_2H_5OH$

Figure 3. The Laplacian of electron density describing the (a) C-H···Cl interaction (calix[4]pyrrole) (b) C-H···Cl interaction (calix[4]arene) (c) C-H···Cl interaction (π-spacer) (d) (a) $Cs^{\cdots}O_C$ interaction of Receptor-$Cs^{+}Cl^{-}$ complex (C/P).